Thin-layer p–n junction fabrication using Ga and In focused ion beam implantation

C-M. Lin and A. J. Steckl
Center for Integrated Electronics and Department of Electrical, Computer and Systems Engineering, Rensselaer Polytechnic Institute, Troy, New York 12181

T. P. Chow
General Electric Co., Corporate Research and Development Center, Schenectady, New York 12301

(Received 20 November 1987; accepted 23 February 1988)

The fabrication of shallow p–n junction impurity profiles using Ga and In focused ion beam (FIB) implantation in conjunction with rapid thermal annealing is reported. A 75-keV focused ion beam with 80 mA/cm^2 current density and 0.5-μm beam diameter was used to implant Ga^+ and In^+ into (100) Si substrates at doses ranging from 1×10^{13} to 5×10^{15}/cm^2. The annealing temperature was varied from 600 to 1000 °C for various times, 10–30 s. Secondary ion mass spectrometry and spreading resistance profiling were used to measure the implanted species atomic and carrier concentration depth profiles. As compared to the conventional broad beam implantation, the FIB implanted Ga concentration depth profiles exhibit higher activation percentage in the end-of-range and tail region. This results in thicker layers and deeper p^+–n junctions, but with lower sheet resistance and leakage current. A similar phenomenon is also observed in In FIB-implanted samples. The damage generated by the high dose rate implantation is possibly responsible for this phenomenon. p^+–n diodes fabricated using Ga FIB doping exhibit very good diode electrical characteristics: ideality factor as low as 1.01, leakage current density below 1 nA/cm^2 at -1 V reverse bias, and breakdown voltage of $\sim$35 V. Diodes fabrication with In generally exhibit shallower junctions, but higher leakage current. Bipolar transistors have been fabricated using FIB-implanted Ga and In thin base layers. Common emitter current gain of 70 and 10 were obtained for Ga and In FIB-implanted bipolar transistors, respectively.

I. INTRODUCTION

Focused ion beam (FIB) technology[1,2] brings a number of advantages to device fabrication, including direct ion doping,[3] lateral doping profiling,[4] and maskless/resistless processing.[5] In this paper, results are presented on the use of Ga and In FIB technology to produce thin-layer p–n junctions for two applications: (a) shallow, heavily doped p^+–n junctions for short-channel metal–oxide semiconductor (MOS) devices; and (b) thin, moderately doped layers for narrow-base bipolar transistors. Ga and In, because of their large mass, have the advantage of a six to eight times shorter range than B, as well as a reduced channeling effect. Historically, Ga and In have not been widely used because of their high diffusivity in SiO_2,[6] and limited solid solubility in Si. However, FIB technology can implement the direct doping of selected regions thus removing the possibility of undesirable Ga and In diffusion through neighboring SiO_2 layers, and its high current density may lead to an enhanced impurity activation.[7,8] In this experiment, all the implantations [FIB and broad beam (BB)] were performed on axis. This condition might become necessary for future generations of submicron devices, since off-axis implantation has recently been reported to result in a shadowing effect which degrades performance for both MOS[9] and bipolar[10] transistors.

Since the current density of FIB implantation is usually 10^4–10^6 times higher than that of conventional broad beam implantation, experimental results for B[7] and Ga[8] FIB implantation have indicated greater damage than conventional implantation. This affects the annealing behavior of the implanted layers. In the case of GaAs, Bamba *et al.*[11] have reported, in a comparison of FIB and BB Si ion implantation, that the concentration tail is longer and thus the junction is deeper for the FIB implantation, with the difference between two implantation methods being the damage which is apparently larger for the FIB implantation. Therefore, the damage created by FIB implantation strongly influences the implanted impurity profile. However, the mechanism is not yet understood. Understanding of this mechanism is imperative, especially when FIB is utilized in small-device fabrication which requires strict control of the impurity profile in both lateral and vertical dimensions.

II. EXPERIMENTS

The focused ion beam experiments were performed using a VG Semicon IBL-100 system. This is a two-lens system which can accelerate singly ionized particles to an energy of 100 keV. The FIB column also includes an $E\times B$ mass filter for use in conjunction with liquid metal alloy sources and a mass quadrupole for *in situ* secondary ion mass spectrometry (SIMS) analysis. A schematic of the system is shown elsewhere.[12]

(100)-oriented 3-in. Si wafers with 3-μm n epilayers (P, 5×10^{15}/cm^3) on n^+ substrates were used. First, the alignment marks for FIB implant were patterned by electron beam (e-beam) lithography and then transferred into the Si wafer via reactive ion etching. For subsequent material analysis, after an 8-nm oxide was thermally grown, areas of 500×500 μm^2 were on-axially implanted with a 75-keV Ga and In FIB at a target current of 200 pA and beam diameter

 © 1988 American Vacuum Society

of 0.5 μm. The current density, defined as target current divided by beam area, was 80 mA/cm^2, in other words, the dose rate was 5×10^{17} ions/cm^2 s. The current density was kept constant throughout this experiment. The implanted doses were generally varied from 1×10^{13} to 1×10^{15}/cm^2, by changing the dwell time for the area from 20 to 2000 s, such that the effective scan rate varied from ~10 to 0.1 cm/s. This is an acceptable means for changing the dose in our experiments, since the scan rate over this range has been shown[8] to have no effect on the FIB Ga activation in Si. For comparison, BB implantations were performed with the same energy of 75 keV, but the current density, 0.8 μA/cm^2, was 10^5 times smaller than for the FIB experiments. Some wafers were preimplanted with Si (80 keV, 2×10^{15}/cm^2) to reduce the channeling effect of the on-axis implantations.

After implantations, samples were rapid thermal annealing (RTA) annealed in a nitrogen ambient using A.G. Associates Heatpulse 410 at temperatures from 600 to 1000 °C for various times. The temperature ramp-up rate was 100–120 °C/s and the ramp-down rate was 50–60 °C/s. After RTA, the samples were divided into two groups: one for SIMS analysis, and another one for spreading resistance profiling (SRP) measurement. From SIMS analysis, the Ga and In atomic depth distribution profiles were obtained. The SIMS analysis was performed using a Cameca IMS-3f ion microscope with a primary beam of 10.5-keV O_2^+ and positive ion spectrometry. The samples which underwent BB implantation with the dose of 1×10^{15}/cm^2 were used as a standard to quantify all the other samples. The carrier concentration depth profiles and the sheet resistance were obtained from SRP measurement.

Taking advantage of FIB direct ion doping process, p^+–n shallow junction diodes and bipolar transistors using a four-level process with e-beam lithography can be fabricated on the same wafer by choosing either high dose for p^+–n diodes or moderate dose for bipolar transistors. Similar to the wafers prepared for material analysis, alignment marks for FIB implantation and e-beam lithography were implemented at the first level, an 8-nm oxide was thermally grown, and then the wafers were loaded into the FIB system. The implantation of the device area was computer controlled by a VAX 11/750 system and performed at the same energy and current density as the previous implants for material analysis. After FIB implantation, the emitter region of the bipolar transistors was defined by the second level and implanted with 30-keV BB As at a dose of 3×10^{15}/cm^2 which results in an emitter depth of 0.1 μm. A 200-nm chemically vapor deposited (CVD) oxide was deposited for passivation and the wafer was RTA annealed first at low temperature (600 °C) for 30 s to induce the solid-phase-epitaxy regrowth and then at higher temperatures (900–1000 °C) for 10 s to remove the implantation damage. The third level defines the contact windows. After oxide etching, Al–1% Si was evaporated for metallization and patterned with the fourth level. A low-temperature sintering step at 300 °C for 15 min was used to improve the Ohmic contact while avoiding aluminum spiking. *I–V* characteristics of the diodes and transistors were measured using Tektronix 576 curve tracer and HP 4140B pA meter.

III. RESULTS AND DISCUSSIONS

A comparison between FIB and BB Ga implantations (with and without Si preimplantation) can be made using the as-implanted SIMS profiles shown in Fig. 1. The beam energy and dose, 75 keV and 1×10^{15}/cm^2, were the same for all three implantations. Except for the Si preimplant, the only difference between these implantations is the dose rate, which is 5×10^{17} ions/cm^2 s for FIB implantations and 5×10^{12} ions/cm^2 s for BB implantations. As expected, all these SIMS profiles have the same peak concentration, 1.6×10^{20}/cm^3, at a depth of 46 nm which is very close to the calculated projected range of 46.5 nm. While the sample with Si preimplant had only a minor deviation ("tail") from a Gaussian profile, tails were seen in the FIB and BB implantation without Si preimplant. The FIB-implanted impurity profile exhibits a deeper tail penetration than the BB-implanted impurity profile. As shown of Fig. 1(b) for FIB implants at doses ranging from 1×10^{13} to 1×10^{15}/cm^2, the long tail is present not only in high-dose implant, but also in low-dose cases, which utilize different scan rates (i.e., dwell times), but the same dose rate. Therefore, it appears that within the range explored the dose rate, rather than the scan rate, is responsible for the long tail.

The carrier concentration profiles of the FIB and BB Ga implanted samples annealed at 600 °C for 30 s are plotted in Fig. 2. The corresponding atomic concentration profiles from SIMS analysis are also included in Fig. 2 to show the

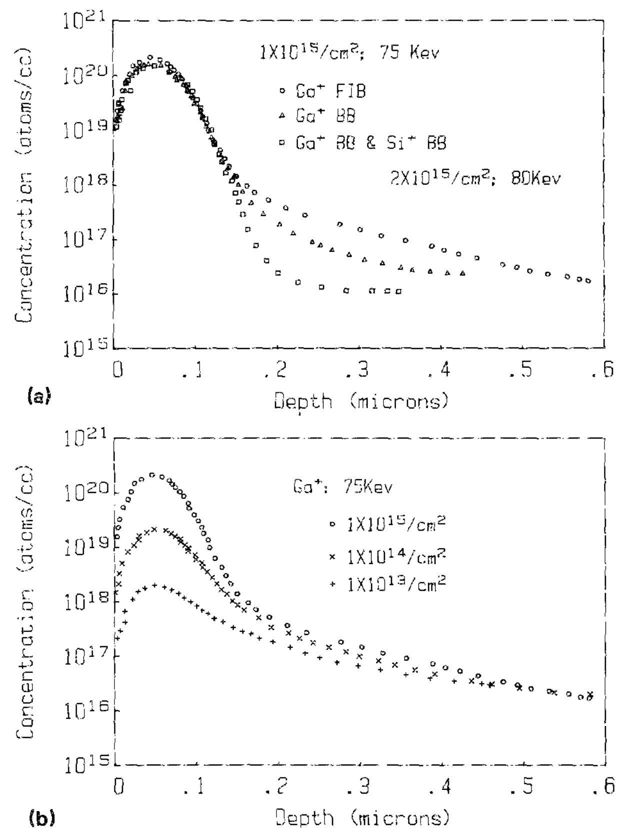

FIG. 1. (a) SIMS profiles of 75-keV Ga FIB and BB (with and without Si preimplant) as-implanted samples at the dose of 1×10^{15}/cm^2. (b) SIMS profiles of Ga FIB as-implanted samples at the doses of 1×10^{13}/cm^2, 1×10^{14}/cm^2, and 1×10^{15}/cm^2.

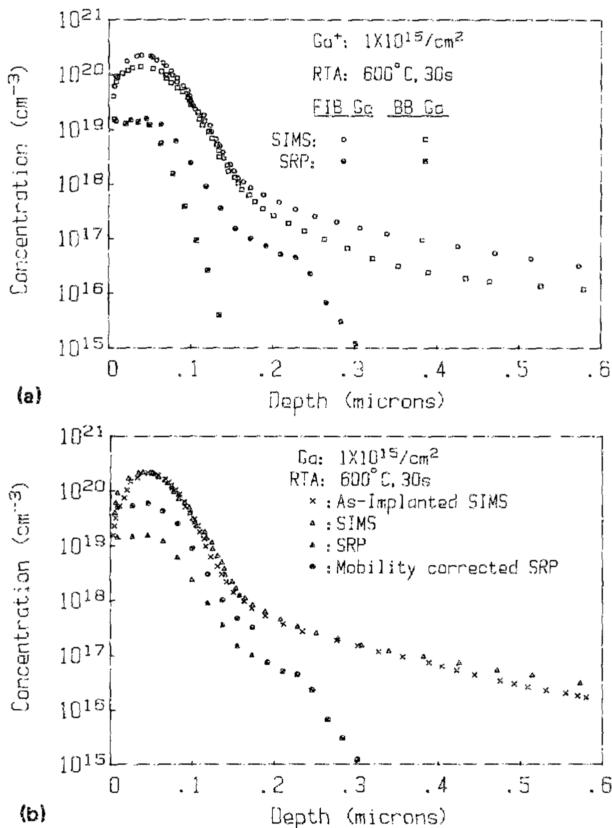

FIG. 2. (a) SIMS and SRP profiles of 75-keV Ga FIB and BB implanted samples RTA-annealed at 600 °C for 30 s, at a dose of $1\times10^{15}/\text{cm}^2$. (b) SIMS and SRP profiles of Ga FIB-implanted sample before and after 600 °C, 30-s RTA, at a dose of $1\times10^{15}/\text{cm}^2$.

difference between the two implantations in the tail region. The implanted dose ($1\times10^{15}/\text{cm}^2$) was higher than the critical dose for amorphizing the Si crystal, which is $2\times10^{14}/\text{cm}^2$ for gallium in Si. Amorphous layers were therefore formed during implantation, and recrystallized in the RTA process leading to an activated impurity concentration higher than the solid solubility at the anneal temperature. The peak carrier concentrations were nearly the same for both FIB- and BB-implanted samples. However, a significantly higher proportion of the implanted tail was activated for the FIB case versus the BB case. This resulted in a junction depth of 0.3 μm for the FIB case and 0.13 μm for the BB case. The junction depth is determined from the SRP profile at the substrate concentration of $5\times10^{15}/\text{cm}^3$. For the low-dose FIB Ga implantations the junction is also deeper than that of the corresponding BB implantation. In general, the activation percentage is clearly higher for the FIB-implanted sample in the end-of-range and tail region. This is presumably due to the larger amount of damage created by the FIB implant. This issue is currently being investigated further in experiments where the FIB scan rate effect is also considered.

In Fig. 2(b), no movement after anneal is observed from the SIMS profile of the FIB Ga-implanted sample before and after 600 °C, 30-s RTA. The carrier concentration in general was converted from the resistivity measured by the SRP technique using the bulk mobility of boron-doped Si crystal. However, the annealing was performed at low temperature (600 °C) for a short time period (30 s), and therefore some damage probably still remains in the Si resulting in lower mobilities than the assumed values. Hence, correction was made using the mobility data from Tsai *et al.*[13] for furnace annealing of 200-keV Ga implantation at the same temperature for 15 min. This leads to a corrected peak carrier concentration of $\sim6\times10^{19}/\text{cm}^3$, which is four to five times higher than the uncorrected value. The SIMS and SRP profiles with high-temperature (1000 °C) RTA were shown in Fig. 3. Although the gallium atomic concentration profiles (SIMS) moved dramatically, the junction depth (SRP) only increased 30 nm. Apparently, the Ga in the tail is not fully activated even for a 1000 °C anneal.

SIMS profiles of In FIB as-implanted samples for doses ranging from 5×10^{13} to $1\times10^{15}/\text{cm}^2$ were obtained. As in the case of Ga FIB implantation, the projected range, 34 nm, is very close to the calculated value of 36 nm for 75-keV In, and the long concentration tails are also observed in these samples. The SIMS and SRP profile of In FIB-implanted samples having the dose of $1\times10^{15}/\text{cm}^2$ and RTA-annealed at 900 °C for 10 s are plotted in Fig. 4. Since indium is not a shallow impurity in Si, the carrier concentrations obtained for the implanted dose are very low ($10^{17}/\text{cm}^3$) giving activation percentages of $<0.1\%$ for both cases.

For the fabrications of the base region of the bipolar transistors, a moderately Ga- and In-doped region ($1-5\times10^{13}/\text{cm}^2$) is required. To verify the impurity profiles of such a thin and moderately doped layer, the SIMS and SRP measurements were performed for the Ga and In FIB-implanted samples annealed at 900 °C for 10 s. From the SRP profile, the junction depths are 0.25 and 0.15 μm, and the average carrier concentration is $\sim2\times10^{17}$ and $5\times10^{16}/\text{cm}^3$, respectively. For an effective emitter junction depth of 0.1 μm, the base width would be 0.15 and 0.05 μm, respectively.

The sheet resistances obtained from SRP measurement are compared for the various temperature regimes for FIB- and BB-implanted samples. The FIB-implanted sample at the dose of $1\times10^{15}/\text{cm}^2$ has the lowest sheet resistance (684

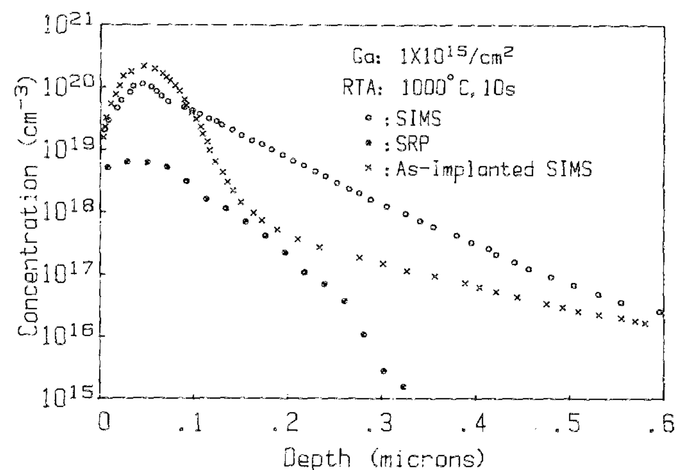

FIG. 3. SIMS and SRP profiles of Ga FIB-implanted sample before and after 1000 °C, 10-s RTA, at a dose of 1×10^{15} cm^2.

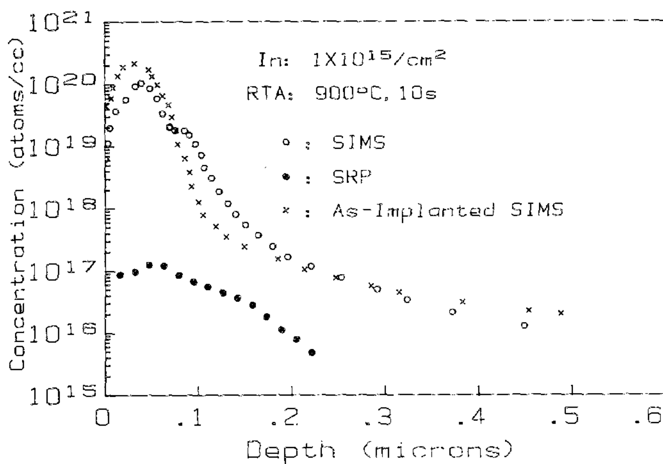

FIG. 4. SIMS and SRP profiles of In FIB-implanted sample before and after 900 °C, 10-s RTA, at a dose of $1\times10^{15}/\text{cm}^2$.

ohm/sq) after annealing at 600 °C for 30 s because the tail was much more activated than for the BB-implanted samples. For In FIB-implanted samples, as mentioned previously, the activation percentage is low, and the sheet resistance varies from 10 kΩ/sq to 100 kΩ/sq at doses ranging from 1×10^{15} to $5\times10^{13}/\text{cm}^2$.

Figure 5 shows the I–V characteristics of two Ga p^+–n diodes with areas of $120\times90\ \mu\text{m}^2$ (diode D5) and $10\times12.5\ \mu\text{m}^2$ (diode B6), and two In p^+–n diodes with areas of $80\times90\ \mu\text{m}^2$ (diode B1) and $10\times32\ \mu\text{m}^2$ (diode B4), respectively. The diodes were FIB implanted at the dose of $1\times10^{15}/\text{cm}^2$, and two-step annealed at 600 °C for 30 s and 900 °C for 10 s. For Ga-implanted diodes, the reverse-bias leakage current density (J_R) at -1 V and ideality factor are 0.9 nA/cm and 1.01 for diode D5, 9.6 nA/cm² and 1.06 for diode B6. The breakdown voltage is 35 V for both diodes. However, the In p^+–n diodes generally exhibit 10–100 times J_R, larger ideality factor of 1.2 to 1.25, and smaller breakdown voltage of 25 to 30 V. To show the effect of edge leakage, the J_R of two sets of Ga p^+–n diodes (annealed at different temperatures) are plotted versus diode perimeter-to-area ratio (L/A) in Fig. 6. J_R is roughly constant for smaller L/A ratio diodes which means that the bulk leakage current component dominates. However, for larger L/A ratio diodes, J_R increases linearly with the L/A ratio and hence is dominated by the edge leakage component. The lowest J_R obtained is 0.9 nA/cm^{-2}. It is interesting to point out that the leakage current of Ga FIB-implanted diodes is greatly reduced as compared to the equivalent BB case.[14]

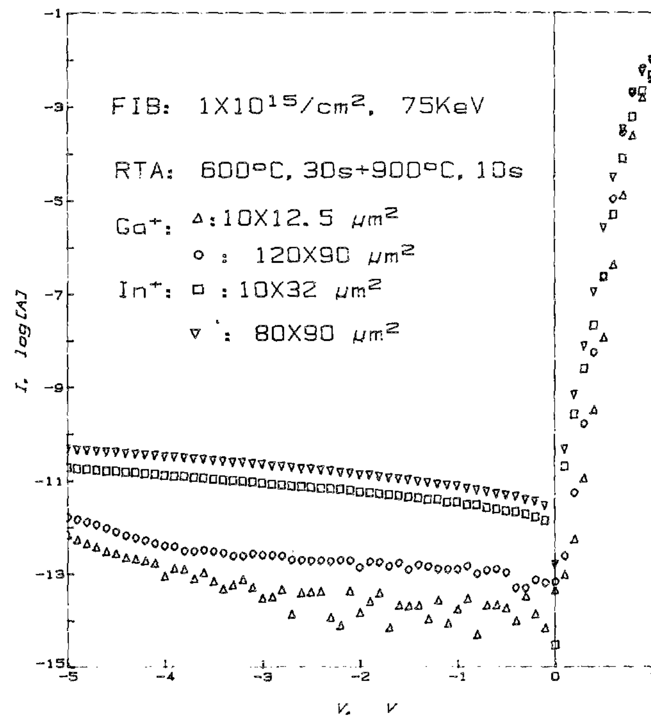

FIG. 5. I–V characteristics of 75-keV Ga and In FIB-implanted p^+–n diodes at a dose of $1\times10^{15}/\text{cm}^2$, and two-step annealed at 600 °C for 30 s and 900 °C for 10 s.

Bipolar transistors were fabricated using FIB-implanted Ga and In moderately doped thin base layers. From SRP measurements, the base widths are 150 and 50 nm for the Ga and In bipolar transistors, respectively. As shown in Figs. 7(a) and 7(b), the common emitter current gain (β) is 70 at a V_{CE} of 8 V for a Ga doped base bipolar transistor. However, β is only 10 for an In doped base bipolar transistor because of its higher junction leakage current. The emitter–collector breakdown voltage is in the range of 15 to 20 V for both transistors.

IV. CONCLUSIONS

In conclusion, shallow junction devices have been fabricated by Ga and In FIB maskless ion implantation with doses from 1×10^{13} to $5\times10^{15}/\text{cm}^2$ at the same dose rate but for different scan rates. A longer atomic concentration tail was observed for FIB vs BB Ga implantation in the as-implanted as well as RTA-annealed SIMS profiles. SRP concentration profiles indicate that the Ga in the end-of-range and tail region is more activated for the FIB case under the anneal conditions studied. This results in a deeper junction depth but with lower sheet resistance and leakage current.

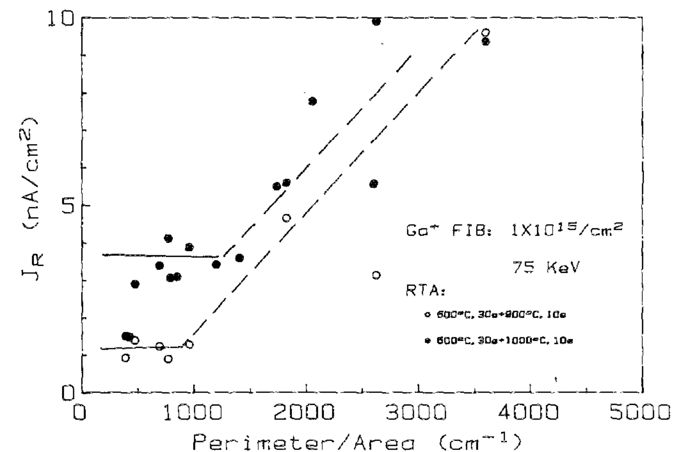

FIG. 6. Reverse-bias leakage current density of Ga FIB-implanted p^+–n junctions vs diode perimeter-to-area (L/A) ratio: ○ Annealed at 600 °C, 30 s + 900 °C, 10 s; ● annealed at 600 °C, 30 s + 1000 °C, 10 s.

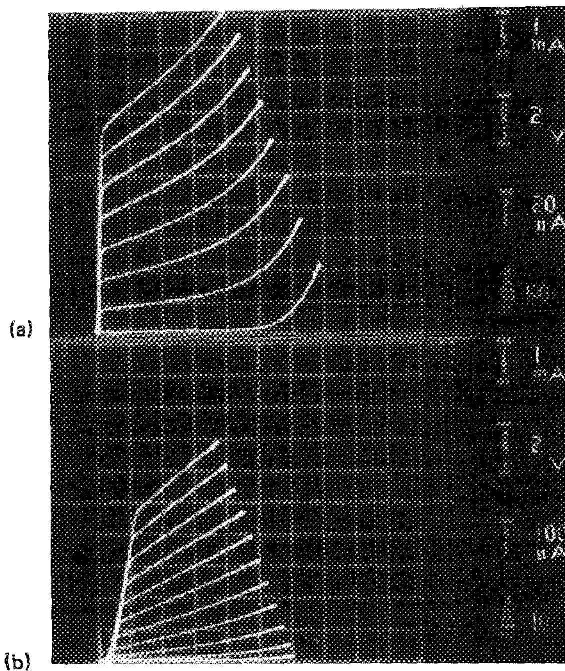

FIG. 7. (a) *I–V* curves of FIB Ga-doped base bipolar transistors. (b) *I–V* curves of FIB In-doped base bipolar transistors.

This phenomenon was observed for both Ga and In implants.

p^+–n diodes and *npn* bipolar transistors were fabricated using Ga and In FIB technology. The *I–V* characteristics of Ga p^+–n diodes show good junction quality with an ideality factor of 1.01, a reverse-bias leakage current of 1 nA/cm^2, and a high breakdown voltage of 35 V. A good current gain of 70 was obtained for the Ga-doped base bipolar transistors. As compared to the Ga *p–n* junction, although the junction is shallower, the In p^+–n diodes exhibit a larger ideality factor of 1.2, a higher reverse-bias leakage current of 100 nA/cm^2, and a smaller breakdown voltage of 30 V. Because the junction was more leaky than the Ga-doped junction, only a small current gain of 10 was obtained for the In-doped base bipolar transistors.

ACKNOWLEDGMENTS

The authors would like to acknowledge partial support for this work from Semiconductor Research Corporation. We thank N. King and M. Bourgeois for the e-beam lithography, and G.A. Smith of General Electric Co. for the SIMS measurements.

[1]V. Wang, J. W. Ward, and R. L. Seliger, J. Vac. Sci. Technol. **19**, 1158 (1981).
[2]A. Wagner, Solid State Technol. **26**, 97 (1983).
[3]R. H. Reuss, D. Morgan, A. Goldenetz, W. M. Clark, D. B. Rensch, and M. Utlaut, J. Vac. Sci. Technol. B **4**, 290 (1986).
[4]S. D. Chu, J. C. Corelli, A. J. Steckl, R. H. Reuss, W. M. Clark, Jr., D. B. Rensch, and W. G. Morris, J. Vac. Sci. Technol. B **4**, 375 (1986).
[5]S. Shukuri, Y. Wada, T. Hagiwara, K. Komori, and M. Tamura, IEEE Trans. Electron Devices **34**, 1264 (1987).
[6]M. Ghezzo and D. M. Brown, J. Electrochem. Soc. **120**, 146 (1973).
[7]M. Tamura, S. Shukuri, T. Ishitani, M. Ichikawa, and T. Doi, Jpn. J. Appl. Phys. **23**, L417 (1984).
[8]M. Tamura, S. Shukuri, M. Moniwa, and M. Default, Appl. Phys. A **39**, 183 (1986).
[9]J. R. Pfiester and F. K. Baker, Tech. Dig. IEDM **87**, 51 (1987).
[10]C. T. Chuang, G. P. Li, and T. H. Ning, IEEE Electron Device Lett. **8**(7), 321 (1987).
[11]V. Bamba, E. Miyauchi, H. Arimoto, K. Kuramoto, A. Takamori, and H. Hashimoto, Jpn. J. Appl. Phys. **24**, L6 (1985).
[12]A. J. Steckl, Proc. IEEE **74**(12), 1753 (1986).
[13]M. Y. Tsai, B. G. Streetman, V. R. Deline, and C. A. Evans, Jr., J. Electron. Mater. **8**(2), 111 (1979).
[14]C.-M. Lin, A. J. Steckl, and T. P. Chow (to be published).